Composite Structures 124 (2015) 283–291

Contents lists available at ScienceDirect

Composite Structures

journal homepage: www.elsevier.com/locate/compstruct

Exact closed-form free vibration analysis for functionally graded micro/nano plates based on modified couple stress and three-dimensional elasticity theories

H. Salehipour, H. Nahvi *, A.R. Shahidi

Department of Mechanical Engineering, Isfahan University of Technology, Isfahan 8415683111, Iran

ARTICLE INFO

Article history:
Available online 19 January 2015

Keywords:
Functionally graded plates
Modified couple stress theory
Three-dimensional elasticity
Free vibration
Analytical modeling

ABSTRACT

In the present manuscript, a model for static and vibration of functionally graded (FG) micro/nano plates is developed based on modified couple stress and three-dimensional elasticity theories. This three-dimensional model contains one length scale parameter to consider the small size effect. The equations of motion and boundary conditions are derived using Hamilton's principle. Analytical closed-form solutions are presented for both in-plane and out-of-plane free vibrations of simply supported plates. To obtain the analytical solutions, elasticity modulus and mass density are assumed to vary exponentially through the plate thickness, while Poisson's ratio and length scale parameter are set to constant values. Finally, some numerical results are presented and the effects of length scale parameter and material gradient index on the natural frequencies for FG micro/nano plates are discussed.

1. Introduction

Micro and nano structures are utilized in many engineering applications, mainly micro- and nano-electro mechanical systems, due to their specific mechanical and physical properties. Experimental results indicate that the influence of small size or Van der Waals forces between atoms become important at micro/nano-scale and so, the classic continuum theory cannot properly predict the mechanical behavior of micro/nano structures. To overcome this problem, different atomistic methods and non-classical continuum models have been developed to capture the size effect at micro/nano-scale. Since the atomistic methods are computationally demanding, non-classical continuum models such as couple stress theory [1–4], strain gradient theory [5], nonlocal elasticity theory [6] and surface elasticity [7] are utilized to study mechanical behavior of micro/nano-scale structures. Modified couple stress is another efficient theory that developed by Yang et al. [8]. The important advantage of this theory over the aforementioned theories, especially the couple stress theory, is that it contains only one material length scale parameter.

Several models have been developed to study bending, vibration and buckling of micro/nano structures, beams and plates, based on the modified couple stress theory. For example, Park and Gao [9] developed a size-dependent Euler–Bernoulli beam model and studied static response of beam under transverse loading. Kong et al. [10] and Kahrobaiyan et al. [11] utilized this model to investigate free vibration and dynamic response of micro/nano beams. Ma et al. [12] considered a Timoshenko beam model to study buckling [13], vibration [14], and the thermal effects on buckling and vibration behavior [15] of microtubes. A Kirchhoff plate model is developed by Tsiatas [16] to analyze bending of microplates. By this model, Yin et al. [17] and Jomehzadeh et al. [18] investigated free vibration of circular and rectangular microplates. Also, Akgoz and Civalek [19] considered free vibration of graphene sheets resting on an elastic matrix known as Pasternak foundation. Ma et al. [20] and Ke et al. [21] separately developed a Mindlin plate model to analyze mechanical behavior of rectangular microplates. The above mentioned works were carried out for homogeneous micro/nano structures. Recently, some researches have been done on the small-scale structures made of FG materials.

FG materials are a new generation of composite materials with many applications in different branches of science and technology. FG materials are composed of at least two constituents, mainly a ceramic and a metal, where their volume fractions vary continuously through the FG material body. This continuity provides soft and continuous stress distribution without the interface difficulties that are common in the laminated composite materials. Recently, FG materials are widely applied in the micro/nano structures and systems such as micro/nano electromechanical systems [22,23], shape memory alloy thin films [24] and atomic force microscopes

* Corresponding author. Tel.: +98 3133915242; fax: +98 3133912628.
E-mail addresses: h.salehipour@me.iut.ac.ir (H. Salehipour), hnahvi@cc.iut.ac.ir (H. Nahvi), shahidi@cc.iut.ac.ir (A.R. Shahidi).

http://dx.doi.org/10.1016/j.compstruct.2015.01.015
0263-8223/

[25]. Based on the modified couple stress theory, some works have been carried out to model and analyze mechanical behavior of FG beams and plates. Asghari et al. [26,27] presented analytical solutions for bending and free vibration of Euler–Bernoulli microbeams with simply supported and clamped boundary conditions, and developed formulations for the size-dependent model of Timoshenko microbeams. Ke et al. [28,29] investigated dynamic stability and nonlinear free vibration of Timoshenko microbeams using numerical method of differential quadrature (DQ). Nonlinear size-dependent models of classic and first-order shear deformation plate theories for axisymmetric bending of circular plates were developed by Reddy and Berry [30]. The models were obtained for power-law variation of the material, temperature-dependent material properties, and the von Kármán geometric nonlinearity. Reddy and Kim [31] developed a general nonlinear third order plate theory based on the von Kármán nonlinear strains using principle of virtual displacements. They assumed that the variation of material properties in the plate thickness obeys a power function. Moreover, they used this model to investigate bending and free vibration of simply supported rectangular plates [32]. Ke et al. [33] studied bending, buckling and free vibration of annular Mindlin microplates using DQ method. The material properties were computed by Mori–Tanaka homogenization technique. Thai et al. [34–36] presented new size-dependent models for static and free vibration of Kirchhoff, Mindlin, Reddy and sinusoidal microplates, and carried out analytical solutions for rectangular plates with simply supported boundary conditions. Simsek and Reddy [37] examined bending and free vibration of microbeams based on various higher order beam theories. Using first-order plate theory, Jung et al. [38,39] investigated buckling, static deformation and free vibration of sigmoid functionally graded material (S-FGM) micro/nano plates embedded in a Pasternak elastic foundation. Ansari et al. [40] utilized generalized differential quadrature (GDQ) method to study vibrational behavior of Mindlin microplates including the von Kármán geometric nonlinearity.

To the authors' best knowledge, no three-dimensional model based on the modified couple stress theory has been reported in the literature for the FG micro/nano plates. The aim of this work is to extract a size-dependent model for bending and free vibration of FG micro/nano plates using the modified couple stress and three-dimensional elasticity theories. The equations of motion and boundary conditions are derived from Hamilton's principle. Then, by assuming exponential variation for the material properties and simply supported boundary conditions, analytical closed-form solutions are obtained for both in-plane and out-of-plane free vibrations of FG micro/nano plates. Finally, numerical results are presented to bring out the influence of material gradient index, length scale parameter and thickness-to-length ratio on the natural frequencies of the FG micro/nano plates.

2. Problem formulation

2.1. Modified couple stress theory

In the modified couple stress theory, the strain energy of a linearly elastic continuum body is defined by a function of both strain tensor and curvature tensor as

$$U = \frac{1}{2}\int_V (\sigma : \varepsilon + m : \chi)dV \tag{1}$$

where σ and ε are the Cauchy stress and Green strain tensors; m is the deviatoric part of couple stress tensor and χ is the symmetric curvature tensor expressed as

$$\chi = \frac{1}{2}\left(\nabla\vec{\theta} + (\nabla\vec{\theta})^T\right) \tag{2a}$$

$$\vec{\theta} = \frac{1}{2}(curl(\vec{u})) \tag{2b}$$

where $\vec{\theta}$ and $\vec{u}$ are the rotation and displacement vectors.

2.2. Equations of motion and boundary conditions

Consider a rectangular FG micro/nano plate with the length of a, width of b and thickness of h. A Cartesian coordinate system (x,y,z) is employed to derive mathematical formulations while x and y coordinates are located in the bottom plane of plate. The equations of motion and boundary conditions of the plate are extracted according to Hamilton's principle given as

$$\int_0^T \delta(K + W - U)dt = 0 \tag{3}$$

in which δK and δU are the virtual kinematic and strain energies, and δW is the virtual work done by the external forces applied on the plate. The virtual kinematic energy is described as

$$\delta K = \int_0^h\int_0^b\int_0^a \rho(z)\left(\frac{\partial u}{\partial t}\delta\left(\frac{\partial u}{\partial t}\right) + \frac{\partial v}{\partial t}\delta\left(\frac{\partial v}{\partial t}\right) + \frac{\partial w}{\partial t}\delta\left(\frac{\partial w}{\partial t}\right)\right)dxdydz \tag{4}$$

where $\rho(z)$ is mass density and u, v and w are components of the displacement vector along the x, y and z axes.

The virtual work done by the external forces and couples expressed are as

$$\begin{aligned}\delta W = &\int_V (f_x\delta u + f_y\delta v + f_z\delta w + c_x\delta\theta_x + c_y\delta\theta_y + c_z\delta\theta_z)dV \\ &+ \int_{\partial V}(q_x\delta u + q_y\delta v + q_z\delta w + s_x\delta\theta_x + s_y\delta\theta_y + s_z\delta\theta_z)dA\end{aligned} \tag{5}$$

in which f_i and c_i ($i = x, y, z$) are the body forces and body couples, respectively; q_i and s_i ($i = x, y, z$) are the tractions and couples applied on the plate surfaces δV (boundary of volume V), respectively.

From Eq. (1), the virtual strain energy is obtained as

$$\begin{aligned}\delta U = &\int_0^h\int_0^b\int_0^a (\sigma_{xx}\delta\varepsilon_{xx} + \sigma_{yy}\delta\varepsilon_{yy} + \sigma_{zz}\delta\varepsilon_{zz} + 2\sigma_{xy}\delta\varepsilon_{xy} \\ &+2\sigma_{xz}\delta\varepsilon_{xz} + 2\sigma_{yz}\delta\varepsilon_{yz})dxdydz \\ &+ \int_0^h\int_0^b\int_0^a \Big(m_{xx}\delta\chi_{xx} + m_{yy}\delta\chi_{yy} + m_{zz}\delta\chi_{zz} \\ &+2m_{xy}\delta\chi_{xy} + 2m_{xz}\delta\chi_{xz} + 2m_{yz}\delta\chi_{yz}\Big)dxdydz \\ = &\int_0^h\int_0^b\int_0^a \left(\sigma_{xx}\frac{\partial\delta u}{\partial x} + \sigma_{yy}\frac{\partial\delta v}{\partial y} + \sigma_{zz}\frac{\partial\delta w}{\partial z}\right. \\ &+\sigma_{xy}\left(\frac{\partial\delta u}{\partial y} + \frac{\partial\delta v}{\partial x}\right) + \sigma_{xz}\left(\frac{\partial\delta u}{\partial z} + \frac{\partial\delta w}{\partial x}\right) \\ &\left.+\sigma_{yz}\left(\frac{\partial\delta v}{\partial z} + \frac{\partial\delta w}{\partial y}\right)\right)dxdydz \\ &+ \int_0^h\int_0^b\int_0^a \left(\frac{m_{xx}}{2}\left(\frac{\partial^2\delta w}{\partial x\partial y} - \frac{\partial^2\delta v}{\partial x\partial z}\right)\right. \\ &+\frac{m_{yy}}{2}\left(\frac{\partial^2\delta u}{\partial y\partial z} - \frac{\partial^2\delta w}{\partial x\partial y}\right) + \frac{m_{zz}}{2}\left(\frac{\partial^2\delta v}{\partial x\partial z} - \frac{\partial^2\delta u}{\partial y\partial z}\right) \\ &+\frac{m_{xy}}{2}\left(\frac{\partial^2\delta w}{\partial y^2} - \frac{\partial^2\delta v}{\partial y\partial z} + \frac{\partial^2\delta u}{\partial x\partial z} - \frac{\partial^2\delta w}{\partial x^2}\right) \\ &+\frac{m_{xz}}{2}\left(\frac{\partial^2\delta w}{\partial y\partial z} - \frac{\partial^2\delta v}{\partial z^2} + \frac{\partial^2\delta v}{\partial x^2} - \frac{\partial^2\delta u}{\partial x\partial y}\right) \\ &\left.+\frac{m_{yz}}{2}\left(\frac{\partial^2\delta u}{\partial z^2} - \frac{\partial^2\delta w}{\partial x\partial z} + \frac{\partial^2\delta v}{\partial x\partial y} - \frac{\partial^2\delta u}{\partial y^2}\right)\right)dxdydz\end{aligned} \tag{6}$$

By substituting δK, δW and δU from Eqs. (4)–(6) into Eq. (3), applying the integration-by-parts and setting the coefficients δu, δv and δw to zero, one can obtain the following three-dimensional equations of motion:

$$\delta u:\frac{\partial\sigma_{xx}}{\partial x}+\frac{\partial\sigma_{xy}}{\partial y}+\frac{\partial\sigma_{xz}}{\partial z}-\frac{1}{2}\frac{\partial^2 m_{yy}}{\partial y\partial z}+\frac{1}{2}\frac{\partial^2 m_{zz}}{\partial y\partial z}-\frac{1}{2}\frac{\partial^2 m_{xy}}{\partial x\partial z}+\frac{1}{2}\frac{\partial^2 m_{xz}}{\partial x\partial y}-\frac{1}{2}\frac{\partial^2 m_{yz}}{\partial z^2}+\frac{1}{2}\frac{\partial^2 m_{yz}}{\partial y^2}+f_x-\frac{1}{2}\frac{\partial c_y}{\partial z}+\frac{1}{2}\frac{\partial c_z}{\partial y}=\rho(z)\frac{\partial^2 u}{\partial t^2} \tag{7a}$$

$$\delta v:\frac{\partial\sigma_{xy}}{\partial x}+\frac{\partial\sigma_{yy}}{\partial y}+\frac{\partial\sigma_{yz}}{\partial z}+\frac{1}{2}\frac{\partial^2 m_{xx}}{\partial x\partial z}-\frac{1}{2}\frac{\partial^2 m_{zz}}{\partial x\partial z}+\frac{1}{2}\frac{\partial^2 m_{xy}}{\partial y\partial z}+\frac{1}{2}\frac{\partial^2 m_{xz}}{\partial z^2}-\frac{1}{2}\frac{\partial^2 m_{xz}}{\partial x^2}-\frac{1}{2}\frac{\partial^2 m_{yz}}{\partial x\partial y}+f_y+\frac{1}{2}\frac{\partial c_x}{\partial z}-\frac{1}{2}\frac{\partial c_z}{\partial x}=\rho(z)\frac{\partial^2 v}{\partial t^2} \tag{7b}$$

$$\delta w:\frac{\partial\sigma_{xz}}{\partial x}+\frac{\partial\sigma_{yz}}{\partial y}+\frac{\partial\sigma_{zz}}{\partial z}-\frac{1}{2}\frac{\partial^2 m_{xx}}{\partial x\partial y}+\frac{1}{2}\frac{\partial^2 m_{yy}}{\partial x\partial y}-\frac{1}{2}\frac{\partial^2 m_{xy}}{\partial y^2}+\frac{1}{2}\frac{\partial^2 m_{xy}}{\partial x^2}-\frac{1}{2}\frac{\partial^2 m_{xz}}{\partial y\partial z}+\frac{1}{2}\frac{\partial^2 m_{yz}}{\partial x\partial z}+f_z-\frac{1}{2}\frac{\partial c_x}{\partial y}+\frac{1}{2}\frac{\partial c_y}{\partial x}=\rho(z)\frac{\partial^2 w}{\partial t^2} \tag{7c}$$

The corresponding boundary conditions are:
at $x = 0, a$:

$$u=0\quad\text{or}\quad \sigma_{xx}-\frac{1}{2}\frac{\partial m_{xy}}{\partial z}+\frac{1}{2}\frac{\partial m_{xz}}{\partial y}-q_x+\frac{1}{2}\frac{\partial s_y}{\partial z}-\frac{1}{2}\frac{\partial s_z}{\partial y}=0 \tag{8a}$$

$$v=0\quad\text{or}\quad \sigma_{xy}+\frac{1}{2}\frac{\partial m_{xx}}{\partial z}-\frac{1}{2}\frac{\partial m_{zz}}{\partial z}-\frac{1}{2}\frac{\partial m_{xz}}{\partial x}-\frac{1}{2}\frac{\partial m_{yz}}{\partial y}-\frac{1}{2}c_z-q_y-\frac{1}{2}\frac{\partial s_x}{\partial z}=0 \tag{8b}$$

$$w=0\quad\text{or}\quad \sigma_{xz}-\frac{1}{2}\frac{\partial m_{xx}}{\partial y}+\frac{1}{2}\frac{\partial m_{yy}}{\partial y}+\frac{1}{2}\frac{\partial m_{xy}}{\partial x}+\frac{1}{2}\frac{\partial m_{yz}}{\partial z}+\frac{1}{2}c_y-q_z+\frac{1}{2}\frac{\partial s_x}{\partial y}=0 \tag{8c}$$

$$\frac{\partial v}{\partial x}=0\quad\text{or}\quad m_{xz}-s_z=0 \tag{8d}$$

$$\frac{\partial w}{\partial x}=0\quad\text{or}\quad m_{xy}-s_y=0 \tag{8e}$$

at $y=0, b$:

$$u=0\quad\text{or}\quad \sigma_{xy}-\frac{1}{2}\frac{\partial m_{yy}}{\partial z}+\frac{1}{2}\frac{\partial m_{zz}}{\partial z}+\frac{1}{2}\frac{\partial m_{xz}}{\partial x}+\frac{1}{2}\frac{\partial m_{yz}}{\partial y}+\frac{1}{2}c_z-q_x+\frac{1}{2}\frac{\partial s_y}{\partial z}=0 \tag{9a}$$

$$v=0\quad\text{or}\quad \sigma_{yy}+\frac{1}{2}\frac{\partial m_{xy}}{\partial z}-\frac{1}{2}\frac{\partial m_{yz}}{\partial x}-q_y-\frac{1}{2}\frac{\partial s_x}{\partial z}+\frac{1}{2}\frac{\partial s_z}{\partial x}=0 \tag{9b}$$

$$w=0\quad\text{or}\quad \sigma_{yz}+\frac{1}{2}\frac{\partial m_{yy}}{\partial x}-\frac{1}{2}\frac{\partial m_{xx}}{\partial x}-\frac{1}{2}\frac{\partial m_{xy}}{\partial y}-\frac{1}{2}\frac{\partial m_{xz}}{\partial z}-\frac{1}{2}c_x-q_z-\frac{1}{2}\frac{\partial s_y}{\partial x}=0 \tag{9c}$$

$$\frac{\partial u}{\partial y}=0\quad\text{or}\quad m_{yz}-s_z=0 \tag{9d}$$

$$\frac{\partial w}{\partial y}=0\quad\text{or}\quad m_{xy}-s_x=0 \tag{9e}$$

at $z=0, h$:

$$u=0\quad\text{or}\quad \sigma_{xz}+\frac{1}{2}\frac{\partial m_{zz}}{\partial y}-\frac{1}{2}\frac{\partial m_{yy}}{\partial y}-\frac{1}{2}\frac{\partial m_{xy}}{\partial x}-\frac{1}{2}\frac{\partial m_{yz}}{\partial z}-\frac{1}{2}c_y-q_x-\frac{1}{2}\frac{\partial s_z}{\partial y}=0 \tag{10a}$$

$$v=0\quad\text{or}\quad \sigma_{yz}-\frac{1}{2}\frac{\partial m_{zz}}{\partial x}+\frac{1}{2}\frac{\partial m_{xx}}{\partial x}+\frac{1}{2}\frac{\partial m_{xz}}{\partial z}+\frac{1}{2}\frac{\partial m_{xy}}{\partial y}+\frac{1}{2}c_x-q_y+\frac{1}{2}\frac{\partial s_z}{\partial x}=0 \tag{10b}$$

$$w=0\quad\text{or}\quad \sigma_{zz}-\frac{1}{2}\frac{\partial m_{xz}}{\partial y}+\frac{1}{2}\frac{\partial m_{yz}}{\partial x}-q_z+\frac{1}{2}\frac{\partial s_x}{\partial y}-\frac{1}{2}\frac{\partial s_y}{\partial x}=0 \tag{10c}$$

$$\frac{\partial u}{\partial z}=0\quad\text{or}\quad m_{yz}-s_y=0 \tag{10d}$$

$$\frac{\partial v}{\partial z}=0\quad\text{or}\quad m_{xz}-s_x=0 \tag{10e}$$

It is noticeable that the surface tractions q_i ($i = x, y, z$) and also surface couples s_i may be different at different boundaries.

Equations of motion (7) are in terms of stress components σ and m. By the three-dimensional linear elasticity and modified couple stress theories,

$$\begin{Bmatrix}\sigma_{xx}\\ \sigma_{yy}\\ \sigma_{zz}\\ \sigma_{xy}\\ \sigma_{xz}\\ \sigma_{yz}\end{Bmatrix}=\frac{E(z)}{1+\nu}\begin{bmatrix}\frac{1-\nu}{1-2\nu} & \frac{\nu}{1-2\nu} & \frac{\nu}{1-2\nu} & 0 & 0 & 0\\ \frac{\nu}{1-2\nu} & \frac{1-\nu}{1-2\nu} & \frac{\nu}{1-2\nu} & 0 & 0 & 0\\ \frac{\nu}{1-2\nu} & \frac{\nu}{1-2\nu} & \frac{1-\nu}{1-2\nu} & 0 & 0 & 0\\ 0 & 0 & 0 & 1 & 0 & 0\\ 0 & 0 & 0 & 0 & 1 & 0\\ 0 & 0 & 0 & 0 & 0 & 1\end{bmatrix}\begin{Bmatrix}\varepsilon_{xx}\\ \varepsilon_{yy}\\ \varepsilon_{zz}\\ \varepsilon_{xy}\\ \varepsilon_{xz}\\ \varepsilon_{yz}\end{Bmatrix} \tag{11a}$$

$$m_{ij}=\frac{E(z)}{1+\nu}l^2\chi_{ij} \tag{11b}$$

here ν and l are Poisson's ratio and material length scale parameter, respectively. These parameters are assumed to be constant through the FG material body. By substituting Eq. (11) into Eq. (7), the equations of motion are obtained in terms of displacements as

$$\begin{aligned}&\frac{E(z)}{2(1+\nu)}\left(\nabla^2 u+\frac{1}{1-2\nu}\frac{\partial^2 u}{\partial x^2}\right)+\frac{E(z)}{2(1+\nu)(1-2\nu)}\left(\frac{\partial^2 v}{\partial x\partial y}+\frac{\partial^2 w}{\partial x\partial z}\right)\\&+\frac{E'(z)}{2(1+\nu)}\left(\frac{\partial u}{\partial z}+\frac{\partial w}{\partial x}\right)\\&-\frac{E(z)}{8(1+\nu)}l^2\left[\frac{\partial^4 u}{\partial y^4}+\frac{\partial^4 u}{\partial z^4}+\frac{\partial^2}{\partial x^2}\left(\frac{\partial^2 u}{\partial y^2}+\frac{\partial^2 u}{\partial z^2}\right)+2\frac{\partial^4 u}{\partial y^2\partial z^2}-\frac{\partial^2}{\partial x\partial y}\left(\nabla^2 v\right)\right.\\&\left.-\frac{\partial^2}{\partial x\partial z}(\nabla^2 w)\right]-\frac{E'(z)}{8(1+\nu)}l^2\left[\frac{\partial}{\partial z}\left(\frac{\partial^2 u}{\partial x^2}+2\frac{\partial^2 u}{\partial y^2}+2\frac{\partial^2 u}{\partial z^2}\right)\right.\\&\left.-\frac{\partial^3 v}{\partial x\partial y\partial z}-\frac{\partial}{\partial x}\left(\nabla^2 w+\frac{\partial^2 w}{\partial z^2}\right)\right]\\&-\frac{E''(z)}{8(1+\nu)}l^2\left[-\frac{\partial^2 u}{\partial y^2}+\frac{\partial^2 u}{\partial z^2}+\frac{\partial}{\partial x}\left(\frac{\partial v}{\partial y}-\frac{\partial w}{\partial z}\right)\right]\\&+f_x-\frac{1}{2}\frac{\partial c_y}{\partial z}+\frac{1}{2}\frac{\partial c_z}{\partial y}=\rho(z)\frac{\partial^2 u}{\partial t^2}\end{aligned} \tag{12a}$$

$$\begin{aligned}&\frac{E(z)}{2(1+\nu)}\left(\nabla^2 v+\frac{1}{1-2\nu}\frac{\partial^2 v}{\partial y^2}\right)+\frac{E(z)}{2(1+\nu)(1-2\nu)}\left(\frac{\partial^2 u}{\partial x\partial y}+\frac{\partial^2 w}{\partial y\partial z}\right)\\&+\frac{E'(z)}{2(1+\nu)}\left(\frac{\partial v}{\partial z}+\frac{\partial w}{\partial y}\right)-\frac{E(z)}{8(1+\nu)}l^2\left[-\frac{\partial^2}{\partial x\partial y}(\nabla^2 u)+\frac{\partial^4 v}{\partial x^4}+\frac{\partial^4 v}{\partial z^4}\right.\\&\left.+2\frac{\partial^4 v}{\partial x^2\partial z^2}+\frac{\partial^2}{\partial y^2}\left(\frac{\partial^2 v}{\partial x^2}+\frac{\partial^2 v}{\partial z^2}\right)-\frac{\partial^2}{\partial y\partial z}(\nabla^2 w)\right]\\&-\frac{E'(z)}{8(1+\nu)}l^2\left[-\frac{\partial^3 u}{\partial x\partial y\partial z}+\frac{\partial}{\partial z}\left(2\frac{\partial^2 v}{\partial x^2}+\frac{\partial^2 v}{\partial y^2}+2\frac{\partial^2 v}{\partial z^2}\right)\right.\\&\left.-\frac{\partial}{\partial y}\left(\nabla^2 w+\frac{\partial^2 w}{\partial z^2}\right)\right]-\frac{E''(z)}{8(1+\nu)}l^2\left[-\frac{\partial^2 v}{\partial x^2}+\frac{\partial^2 v}{\partial z^2}+\frac{\partial}{\partial y}\left(\frac{\partial u}{\partial x}-\frac{\partial w}{\partial z}\right)\right]\\&+f_y+\frac{1}{2}\frac{\partial c_x}{\partial z}-\frac{1}{2}\frac{\partial c_z}{\partial x}=\rho(z)\frac{\partial^2 v}{\partial t^2}\end{aligned} \tag{12b}$$

$$\frac{E(z)}{2(1+v)}\left(\nabla^2 w+\frac{1}{1-2v}\frac{\partial^2 w}{\partial z^2}\right)+\frac{E(z)}{2(1+v)(1-2v)}\left(\frac{\partial^2 u}{\partial x\partial z}+\frac{\partial^2 v}{\partial y\partial z}\right)$$
$$+\frac{E'(z)}{(1+v)(1-2v)}\left((1-v)\frac{\partial w}{\partial z}+v\left(\frac{\partial u}{\partial x}+\frac{\partial v}{\partial y}\right)\right)$$
$$-\frac{E(z)}{8(1+v)}l^2\left[-\frac{\partial^2}{\partial x\partial z}(\nabla^2 u)-\frac{\partial^2}{\partial y\partial z}(\nabla^2 v)+\frac{\partial^4 w}{\partial x^4}+\frac{\partial^4 w}{\partial y^4}\right.$$
$$\left.+2\frac{\partial^4 w}{\partial x^2\partial y^2}+\frac{\partial^2}{\partial z^2}\left(\frac{\partial^2 w}{\partial x^2}+\frac{\partial^2 w}{\partial y^2}\right)\right]$$
$$-\frac{E'(z)}{8(1+v)}l^2\left[-\frac{\partial^2}{\partial z^2}\left(\frac{\partial u}{\partial x}+\frac{\partial v}{\partial y}\right)+\frac{\partial}{\partial z}\left(\frac{\partial^2 w}{\partial x^2}+\frac{\partial^2 w}{\partial y^2}\right)\right]$$
$$+f_z-\frac{1}{2}\frac{\partial c_x}{\partial y}+\frac{1}{2}\frac{\partial c_y}{\partial x}=\rho(z)\frac{\partial^2 w}{\partial t^2} \quad (12c)$$

where ∇^2 denotes the Laplacian operator given as

$$\nabla^2=\frac{\partial^2}{\partial x^2}+\frac{\partial^2}{\partial y^2}+\frac{\partial^2}{\partial z^2} \quad (13)$$

2.3. Free vibration analysis

In this section, analytical closed-form solutions are presented for both in-plane and out-of-plane free vibrations of simply supported FG micro/nano plates. In order to obtain analytical solutions, the elasticity modulus and mass density are assumed to have the following exponential distributions:

$$E(z)=E_0\exp(\phi z) \quad (14a)$$

$$\rho(z)=\rho_0\exp(\phi z) \quad (14b)$$

where E_0 and ρ_0 are the elasticity modulus and mass density at the bottom surface, and ϕ is the material gradient index. For the plate with simply supported boundary conditions, the displacement components are expressed as

$$u=f(z)\sum_{n=1}^{\infty}\sum_{m=1}^{\infty}\alpha_m\cos(\alpha_m x)\sin(\beta_n y)e^{j\omega_{m,n}^q t} \quad (15a)$$

$$v=g(z)\sum_{n=1}^{\infty}\sum_{m=1}^{\infty}\beta_n\sin(\alpha_m x)\cos(\beta_n y)e^{j\omega_{m,n}^q t} \quad (15b)$$

$$w=k(z)\sum_{n=1}^{\infty}\sum_{m=1}^{\infty}\sin(\alpha_m x)\sin(\beta_n y)e^{j\omega_{m,n}^q t} \quad (15c)$$

in which $j=\sqrt{-1}, \alpha_m=m\pi/a, \beta_n=n\pi/b. \omega_{m,n}^q$ is the natural frequency and m, n and q are the number of mode shapes along the directions of Cartesian coordinate. Further, the functions $f(z)$, $g(z)$ and $k(z)$ express the variations of displacement components through the plate thickness and t is the time variable. In the absence of external forces and couples, the displacements in Eq. (15) satisfy the following simply supported boundary conditions obtained from Eqs. (8) and (9):

$$v=w=m_{xy}=m_{xz}=\sigma_{xx}-\frac{1}{2}\frac{\partial m_{xy}}{\partial z}+\frac{1}{2}\frac{\partial m_{xz}}{\partial y}=0 \quad \text{at} \quad x=0,a \quad (16a)$$

$$u=w=m_{xy}=m_{yz}=\sigma_{yy}+\frac{1}{2}\frac{\partial m_{xy}}{\partial z}-\frac{1}{2}\frac{\partial m_{yz}}{\partial x}=0 \quad \text{at} \quad y=0,b \quad (16b)$$

Substitution of the displacement components from Eq. (15) and material properties from Eq. (14) into the equations of motion (12) and simplifying the results lead to the following three ordinary differential equations:

$$A_1f^4(z)+2\phi A_1f'''(z)+(A_2+\alpha_m^2A_1)f''(z)+(A_3+\alpha_m^2\phi A_1)f'(z)$$
$$+A_4f(z)+\beta_n^2A_1g''(z)+\beta_n^2\phi A_1g'(z)-\beta_n^2A_6g(z)-A_1k'''(z)$$
$$-2\phi A_1k''(z)+A_7k'(z)+A_8k(z)=0 \quad (17a)$$

$$A_1g^4(z)+2\phi A_1g'''(z)+(A_2+\beta_n^2A_1)g''(z)+(A_3+\beta_n^2\phi A_1)g'(z)$$
$$+A_5g(z)+\alpha_m^2A_1f''(z)+\alpha_m^2\phi A_1f'(z)-\alpha_m^2A_6f(z)-A_1k'''(z)$$
$$-2\phi A_1k''(z)+A_7k'(z)+A_8k(z)=0 \quad (17b)$$

$$C_1k''(z)+\phi C_1k'(z)+C_2k(z)+\alpha_m^2(C_3f'''(z)+\phi C_3f''(z)+C_4f'(z)$$
$$+C_5f(z))+\beta_n^2(C_3g'''(z)+\phi C_3g''(z)+C_4g'(z)+C_5g(z))=0 \quad (17c)$$

where

$$A_1=C_3=-\frac{E_0l^2}{8(1+v)}$$

$$A_2=\frac{E_0}{2(1+v)}+\frac{E_0l^2\gamma_{mn}}{4(1+v)}-\frac{E_0l^2\phi^2}{8(1+v)}$$

$$A_3=\frac{E_0\phi}{2(1+v)}+\frac{E_0l^2\phi\gamma_{mn}}{4(1+v)}$$

$$\begin{Bmatrix}A_4\\A_5\end{Bmatrix}=-\frac{E_0(1-v)}{(1+v)(1-2v)}\begin{Bmatrix}\alpha_m^2\\\beta_n^2\end{Bmatrix}-\left(\frac{E_0}{2(1+v)}+\frac{E_0l^2\gamma_{mn}}{8(1+v)}+\frac{E_0l^2\phi^2}{8(1+v)}\right)\begin{Bmatrix}\beta_n^2\\\alpha_m^2\end{Bmatrix}+\rho_0\omega^2$$

$$\begin{Bmatrix}A_6\\A_7\end{Bmatrix}=\frac{E_0v}{(1+v)(1-2v)}+\frac{E_0}{2(1+v)}-\frac{E_0l^2\gamma_{mn}}{8(1+v)}+\begin{Bmatrix}-1\\1\end{Bmatrix}\frac{E_0l^2\phi^2}{8(1+v)}$$

$$A_8=\frac{E_0\phi}{2(1+v)}-\frac{E_0l^2\phi\gamma_{mn}}{8(1+v)}$$

$$C_1=\frac{E_0(1-v)}{(1+v)(1-2v)}+\frac{E_0l^2\gamma_{mn}}{8(1+v)}$$

$$C_2=-\frac{E_0\gamma_{mn}}{2(1+v)}-\frac{E_0l^2\gamma_{mn}^2}{8(1+v)}+\rho_0\omega^2$$

$$C_4=-\frac{E_0v}{(1+v)(1-2v)}-\frac{E_0}{2(1+v)}+\frac{E_0l^2\gamma_{mn}}{8(1+v)} \quad (18a)$$

$$C_5=-\frac{E_0v\phi}{(1+v)(1-2v)}$$

and

$$\gamma_{mn}=\alpha_m^2+\beta_n^2 \quad (18b)$$

Also for the free vibration, Eq. (15) should satisfy free boundary conditions on the top and bottom plate surfaces obtained from Eq. (10) as

$$\left[\sigma_{xz}+\frac{1}{2}\frac{\partial m_{zz}}{\partial y}-\frac{1}{2}\frac{\partial m_{yy}}{\partial y}-\frac{1}{2}\frac{\partial m_{xy}}{\partial x}-\frac{1}{2}\frac{\partial m_{yz}}{\partial z}\right]\Bigg|_{z=0,h}=0 \quad (19a)$$

$$\left[\sigma_{yz}-\frac{1}{2}\frac{\partial m_{zz}}{\partial x}+\frac{1}{2}\frac{\partial m_{xx}}{\partial x}+\frac{1}{2}\frac{\partial m_{xz}}{\partial z}+\frac{1}{2}\frac{\partial m_{xy}}{\partial y}\right]\Bigg|_{z=0,h}=0 \quad (19b)$$

$$\left[\sigma_{zz} - \frac{1}{2}\frac{\partial m_{xz}}{\partial y} + \frac{1}{2}\frac{\partial m_{yz}}{\partial x}\right]\Big|_{z=0,h} = 0 \tag{19c}$$

$$m_{xz}|_{z=0,h} = m_{yz}|_{z=0,h} = 0 \tag{19d}$$

Substitution of Eq. (15) into Eq. (19) and simplifying, results in the following equations:

$$\begin{aligned}&\Big[E(z)(f'(z)+k(z)) + \frac{E(z)l^2}{4}(-f'''(z) + (\gamma_{mn}+2\beta_n^2)f'(z)\\ &-\gamma_{mn}k(z) + k''(z) - 2\beta_n^2 g'(z))\\ &-\frac{E'(z)l^2}{4}(-\beta_n^2(g(z)-f(z)) + f''(z) - k'(z))\Big]\Big|_{z=0,h} = 0\end{aligned} \tag{20a}$$

$$\begin{aligned}&\Big[E(z)(g'(z)+k(z)) + \frac{E(z)l^2}{4}(-g'''(z) + (2\alpha_m^2+\gamma_{mn})g'(z) - \gamma_{mn}k(z)\\ &+k''(z) - 2\alpha_m^2 f'(z))\\ &-\frac{E'(z)l^2}{4}(-\alpha_m^2(f(z)-g(z)) + g''(z) - k'(z))\Big]\Big|_{z=0,h} = 0\end{aligned} \tag{20b}$$

$$\begin{aligned}E(z)&\Big[\frac{1}{1-2\nu}((1-\nu)k'(z) - \nu\alpha_m^2 f(z) - \nu\beta_n^2 g(z))\\ &+\frac{l^2}{8}(\gamma_{mn}k'(z) - \alpha_m^2 f''(z) - \beta_n^2 g''(z))\Big]\Big|_{z=0,h} = 0\end{aligned} \tag{20c}$$

$$E(z)l^2\left[-\alpha_m^2(f(z)-g(z)) + g''(z) - k'(z)\right]|_{z=0,h} = 0 \tag{20d}$$

$$E(z)l^2\left[-\beta_n^2(g(z)-f(z)) + f''(z) - k'(z)\right]|_{z=0,h} = 0 \tag{20e}$$

2.3.1. In-plane modes

For the in-plane free vibration, the general solution of Eq. (17) is found as

$$\begin{Bmatrix} f(z)\\ g(z)\\ k(z)\end{Bmatrix} = \begin{Bmatrix} F\\ G\\ 0\end{Bmatrix}\exp(\lambda z) \tag{21}$$

By using Eq. (21) into Eq. (17c), $g(z)$ is found in the form of

$$g(z) = -\frac{\alpha_m^2}{\beta_n^2}f(z) \tag{22}$$

By substituting Eqs. (21) and (22) into Eqs. (17a) and (17b) and simplifying, only one independent characteristic equation is obtained as

$$A_1\lambda^4 + 2\phi A_1\lambda^3 + A_2\lambda^2 + A_3\lambda + A_9 = 0 \tag{23}$$

where

$$A_9 = A_4 + \alpha_m^2 A_6 \tag{24}$$

From this equation, four roots are obtained as

$$\begin{Bmatrix}\lambda_1\\ \lambda_2\\ \lambda_3\\ \lambda_4\end{Bmatrix} = -\frac{\phi}{2} \pm \sqrt{\frac{\phi^2}{4} + \frac{2+l^2\gamma_{mn}}{l^2} \pm \sqrt{\frac{E_0\left(4 - l^4\phi^2\gamma_{mn}\right) + 8l^2\rho_0\omega^2(1+\nu)}{E_0 l^4}}} \tag{25}$$

The roots of Eq. (25) can be real or complex. For the real values, we get

$$f(z) = F_1\exp(\lambda_1 z) + F_2\exp(\lambda_2 z) + F_3\exp(\lambda_3 z) + F_4\exp(\lambda_4 z) \tag{26a}$$

$$g(z) = -\frac{\alpha_m^2}{\beta_n^2}(F_1\exp(\lambda_1 z) + F_2\exp(\lambda_2 z) + F_3\exp(\lambda_3 z) + F_4\exp(\lambda_4 z)) \tag{26b}$$

Eq. (26) should satisfy the surface boundary conditions given in Eq. (20). Introducing Eq. (26) into Eq. (20) yields four independent algebraic equations in terms of F_i ($\{i = 1, 2, 3, 4\}$) as

$$\begin{aligned}E(z)\Big[&\left(3l^2\gamma_{mn} - l^2\lambda_1^2 + 4\right)\lambda_1 F_1\exp(\lambda_1 z)\\ &+\left(3l^2\gamma_{mn} - l^2\lambda_2^2 + 4\right)\lambda_2 F_2\exp(\lambda_2 z)\\ &+\left(3l^2\gamma_{mn} - l^2\lambda_3^2 + 4\right)\lambda_3 F_3\exp(\lambda_3 z)\\ &+\left(3l^2\gamma_{mn} - l^2\lambda_4^2 + 4\right)\lambda_4 F_4\exp(\lambda_4 z)\Big]\Big|_{z=0,h} = 0\end{aligned} \tag{27a}$$

$$\begin{aligned}E(z)l^2&\left[(\gamma_{mn}+\lambda_1^2)F_1\exp(\lambda_1 z) + (\gamma_{mn}+\lambda_2^2)F_2\exp(\lambda_2 z)\right.\\ &\left.+(\gamma_{mn}+\lambda_3^2)F_3\exp(\lambda_3 z) + (\gamma_{mn}+\lambda_4^2)F_4\exp(\lambda_4 z)\right]\big|_{z=0,h} = 0\end{aligned} \tag{27b}$$

The set of algebraic Eq. (27) has a nonzero solution when the determinant of coefficient matrix is equal to zero. By setting the determinant to zero, the natural frequencies of the in-plane vibration modes are extracted.

For the complex roots of Eq. (25), $f(z)$ and $g(z)$ should be changed accordingly. But, for the sake of brevity, the new equations are not presented here. The rest of solution procedure is the same as that explained.

2.3.2. Out-of-plane modes

For the out-of-plane modes, the solution of Eq. (17) has the following form:

$$\begin{Bmatrix} f(z)\\ g(z)\\ k(z)\end{Bmatrix} = \begin{Bmatrix} F\\ G\\ K\end{Bmatrix}\exp(\lambda z) \tag{28}$$

By substituting Eq. (28) into Eqs. (17a) and (17b), coefficients F and G are obtained as

$$F = G = \frac{A_1\lambda^3 + 2\phi A_1\lambda^2 - A_7\lambda - A_8}{A_1\lambda^4 + 2\phi A_1\lambda^3 + (\gamma_{mn}A_1 + A_2)\lambda^2 + (\gamma_{mn}\phi A_1 + A_3)\lambda + A_4 - \beta_n^2 A_6}K \tag{29}$$

From Eqs. (28), (29) and (17c), the following characteristic equation is derived:

$$\begin{aligned}&A_1(C_1+\gamma_{mn}C_3)\lambda^6 + 3\phi A_1(C_1+\gamma_{mn}C_3)\lambda^5\\ &+(\gamma_{mn}A_1C_1 + A_2C_1 + 2\phi^2A_1C_1 + A_1C_2 - \gamma_{mn}A_7C_3\\ &+\gamma_{mn}A_1C_4 + 2\gamma_{mn}\phi^2A_1C_3)\lambda^4 + (2\gamma_{mn}\phi A_1C_1 + A_3C_1\\ &+\phi A_2C_1 + 2\phi A_1C_2 - \gamma_{mn}A_8C_3 - \gamma_{mn}\phi A_7C_3\\ &+2\gamma_{mn}\phi A_1C_4 + \gamma_{mn}A_1C_5)\lambda^3\\ &+(A_4C_1 - \beta_n^2A_6C_1 + \gamma_{mn}\phi^2A_1C_1 + \phi A_3C_1 + \gamma_{mn}A_1C_2\\ &+A_2C_2 - \gamma_{mn}\phi A_8C_3 - \gamma_{mn}A_7C_4 + 2\gamma_{mn}\phi A_1C_5)\lambda^2\\ &+(\phi A_4C_1 - \phi\beta_n^2A_6C_1 + \gamma_{mn}\phi A_1C_2 + A_3C_2 - \gamma_{mn}A_8C_4 - \gamma_{mn}A_7C_5)\lambda\\ &+A_4C_2 - \beta_n^2A_6C_2 - \gamma_{mn}A_8C_5 = 0\end{aligned} \tag{30}$$

This equation has six roots $\lambda_i (i = 1, 2, \ldots, 6)$.

Thus, the functions $f(z)$, $g(z)$ and $k(z)$ are expressed as

$$\begin{aligned}f(z) = &F_1\exp(\lambda_1 z) + F_2\exp(\lambda_2 z) + F_3\exp(\lambda_3 z) + F_4\exp(\lambda_4 z)\\ &+F_5\exp(\lambda_5 z) + F_6\exp(\lambda_6 z)\end{aligned} \tag{31a}$$

$$g(z) = G_1\exp(\lambda_1 z) + G_2\exp(\lambda_2 z) + G_3\exp(\lambda_3 z) + G_4 \times \exp(\lambda_4 z) + G_5\exp(\lambda_5 z) + G_6\exp(\lambda_6 z) \quad (31b)$$

$$k(z) = K_1\exp(\lambda_1 z) + K_2\exp(\lambda_2 z) + K_3\exp(\lambda_3 z) + K_4 \times \exp(\lambda_4 z) + K_5\exp(\lambda_5 z) + K_6\exp(\lambda_6 z) \quad (31c)$$

where

$$F_i = G_i = \eta_i K_i, \quad (i = 1, 2, \ldots, 6)$$
$$\eta_i = \frac{(A_1\lambda_i^3 + 2\phi A_1\lambda_i^2 - A_7\lambda_i - A_8)}{A_1\lambda_i^4 + 2\phi A_1\lambda_i^3 + (\gamma_{mn}A_1 + A_2)\lambda_i^2 + (\gamma_{mn}\phi A_1 + A_3)\lambda_i + A_4 - \beta_n^2 A_6} \quad (32)$$

To extract the natural frequencies of the out-of-plane modes, the boundary conditions at the top and bottom surfaces of plate, Eq. (20), should be satisfied by the functions given in Eq. (31). Using Eq. (31) into Eq. (20), the following six independent equations are obtained:

$$\begin{aligned} E(z)\Big[&\Big(4\eta_1\lambda_1 + 4 - l^2\lambda_1^2(\eta_1\lambda_1 - 1) + l^2\gamma_{mn}(\eta_1\lambda_1 - 1)\Big)K_1\exp(\lambda_1 z) \\ &+ \Big(4\eta_2\lambda_2 + 4 - l^2\lambda_2^2(\eta_2\lambda_2 - 1) + l^2\gamma_{mn}(\eta_2\lambda_2 - 1)\Big)K_2\exp(\lambda_2 z) \\ &+ \Big(4\eta_3\lambda_3 + 4 - l^2\lambda_3^2(\eta_3\lambda_3 - 1) + l^2\gamma_{mn}(\eta_3\lambda_3 - 1)\Big)K_3\exp(\lambda_3 z) \\ &+ \Big(4\eta_4\lambda_4 + 4 - l^2\lambda_4^2(\eta_4\lambda_4 - 1) + l^2\gamma_{mn}(\eta_4\lambda_4 - 1)\Big) \times K_4\exp(\lambda_4 z) \\ &+ \Big(4\eta_5\lambda_5 + 4 - l^2\lambda_5^2(\eta_5\lambda_5 - 1) + l^2\gamma_{mn}(\eta_5\lambda_5 - 1)\Big)K_5\exp(\lambda_5 z) \\ &+ \Big(4\eta_6\lambda_6 + 4 - l^2\lambda_6^2(\eta_6\lambda_6 - 1) + l^2\gamma_{mn}(\eta_6\lambda_6 - 1)\Big)K_6\exp(\lambda_6 z)\Big]\Big|_{z=0,h} = 0 \end{aligned} \quad (33a)$$

$$\begin{aligned} E(z)[&((1-\nu)\lambda_1 - \nu\gamma_{mn}\eta_1)K_1\exp(\lambda_1 z) \\ &+ ((1-\nu)\lambda_2 - \nu\gamma_{mn}\eta_2)K_2\exp(\lambda_2 z) \\ &+ ((1-\nu)\lambda_3 - \nu\gamma_{mn}\eta_3)K_3\exp(\lambda_3 z) \\ &+ ((1-\nu)\lambda_4 - \nu\gamma_{mn}\eta_4)K_4\exp(\lambda_4 z) \\ &+ ((1-\nu)\lambda_5 - \nu\gamma_{mn}\eta_5)K_5\exp(\lambda_5 z) \\ &+ ((1-\nu)\lambda_6 - \nu\gamma_{mn}\eta_6)K_6\exp(\lambda_6 z)]|_{z=0,h} = 0 \end{aligned} \quad (33b)$$

$$\begin{aligned} E(z)l^2\big[&(\lambda_1^2\eta_1 - \lambda_1)K_1\exp(\lambda_1 z) + (\lambda_2^2\eta_2 - \lambda_2)K_2\exp(\lambda_2 z) \\ &+ (\lambda_3^2\eta_3 - \lambda_3)K_3\exp(\lambda_3 z) + (\lambda_4^2\eta_4 - \lambda_4)K_4\exp(\lambda_4 z) \\ &+ (\lambda_5^2\eta_5 - \lambda_5)K_5\exp(\lambda_5 z) + (\lambda_6^2\eta_6 - \lambda_6)K_6\exp(\lambda_6 z)\big]\big|_{z=0,h} = 0 \end{aligned} \quad (33c)$$

Nontrivial solution, $K_i \neq 0$, to the set of Eq. (33) leads to a characteristic equation, from the solution which the natural frequencies of the out-of-plane modes are extracted.

It is noticeable that for the non-real values of the roots, Eq. (31) must be changed accordingly. But, to avoid lengthiness, the new forms of Eq. (31) are not presented. The rest of solution method is the same as that explained.

3. Numerical examples

In order to present numerical results in a comparable form, the following non-dimensional parameters are defined:

$$\bar{\phi} = E_h/E_0 = \exp(\phi h) \quad (34a)$$

$$\bar{l} = l/h \quad (34b)$$

$$\bar{\omega}_{m,n}^q = \omega_{m,n}^q a^2\sqrt{\rho/E}\Big/h \quad (34c)$$

where E_h is the elasticity modulus at the top surface of plate.

Using the modified couple stress theory, no results have been published in the literatures for the free vibration of FG plates with exponential distribution of the material properties. Hence, the comparison results are presented for the homogeneous cases. The first non-dimensional natural frequency $\bar{\omega}_{1,1}^1$ of a square homogeneous plate is tabulated in Table 1 and compared with the results of two-dimensional theories for different length scale parameters and length-to-thickness ratios. As the table shows, the differences between the results of present three-dimensional solution and those of two-dimensional theories significantly decrease when the length-to-thickness ratio increases.

Tables 2 and 3 list the first and second non-dimensional frequencies of the square FG micro/nano plates for the out-of-plane and in-plane modes, respectively. The results are obtained for the length-to-thickness ratios of 5 and 10, and different values of length scale parameter $\bar{l}$ and gradient index $\bar{\phi}$. The Poisson's ratio is taken as 0.3 throughout the numerical results. It can be observed that with an increase in the length scale parameter, the frequencies of the out-of-plane modes rise. This originates from the significant increase of the plate flexural stiffness. But, the increasing the shear stiffness is very less when compared to the flexural stiffness. This is deduced from the small variations of frequencies for the in-plane modes versus the length scale parameter.

To show the effects of length scale parameter and gradient index, variation of first non-dimensional frequency of the out-of-

Table 1
Comparison of the first non-dimensional natural frequency $\omega_{1,1}^1$ of a homogeneous micro/nano plate.

a/h	$\bar{l}$	Present ($\nu = 0.3$)	HSDT [34] ($\nu = 0.3$)	Present ($\nu = 0.38$)	FSDT [33] ($\nu = 0.38$)	CPT [33] ($\nu = 0.38$)
5	0	5.3036	5.2813	5.4205	5.3871	5.9671
	0.2	5.7560	5.7699	5.8324	5.7797	6.3957
	0.4	6.8966	7.0330	6.8849	6.7996	7.5366
	0.6	8.3932	8.7389	8.2850	8.1595	9.1264
	0.8	10.021	10.6766	9.8232	9.6451	10.9718
	1	11.654	12.7408	11.376	11.1311	12.9640
10	0	5.7769	5.7694	5.9412	5.9301	6.1103
	0.2	6.2495	6.2537	6.3736	6.3559	6.5491
	0.4	7.4765	7.5210	7.5102	7.4807	7.7174
	0.6	9.1389	9.2543	9.0713	9.0261	9.3453
	0.8	11.017	11.2396	10.852	10.7848	11.2349
	1	12.988	13.3651	12.733	12.6360	13.2749
20	0	5.9219	5.9199	6.1027	6.0997	6.1477
	0.2	6.4016	6.4027	6.5425	6.5376	6.5892
	0.4	7.6587	7.6708	7.7091	7.7009	7.7646
	0.6	9.3801	9.4116	9.3285	9.3158	9.4026
	0.8	11.349	11.4108	11.199	11.1801	11.3037
	1	13.450	13.5545	13.207	13.1786	13.3562

Table 2
First and second non-dimensional natural frequencies of the out-of-plane modes for square FG plates.

$\bar{\phi}$	$\bar{l}$	a/h = 5		a/h = 10	
		$\omega_{1,1}^1$	$\omega_{2,1}^1$	$\omega_{1,1}^1$	$\omega_{2,1}^1$
1	0	5.3036	11.645	5.7769	13.805
	0.2	5.7560	12.726	6.2495	14.958
	0.4	6.8966	15.346	7.4765	17.904
	0.6	8.3932	18.643	9.1389	21.825
	0.8	10.021	22.057	11.017	26.163
	1	11.654	25.270	12.988	30.605
5	0	5.0168	11.073	5.4392	13.032
	0.2	5.5043	12.255	5.9424	14.268
	0.4	6.7133	15.055	7.2307	17.377
	0.6	8.2707	18.492	8.9499	21.449
	0.8	9.9435	21.991	10.872	25.901
	1	11.607	25.248	12.876	30.426
10	0	4.7524	10.545	5.1295	12.320
	0.2	5.2745	11.824	5.6635	13.638
	0.4	6.5480	14.791	7.0109	16.904
	0.6	8.1611	18.356	8.7827	21.114
	0.8	9.8741	21.932	10.744	25.669
	1	11.566	25.229	12.779	30.268

Table 3
First and second non-dimensional natural frequencies of the in-plane modes for square FG plates.

$\bar{\phi}$	$\bar{l}$	a/h = 5		a/h = 10	
		$\omega_{1,1}^2$	$\omega_{2,1}^2$	$\omega_{1,1}^2$	$\omega_{2,1}^2$
1	0	13.777	21.783	27.554	43.566
	0.2	13.820	21.956	27.575	43.652
	0.4	13.913	22.344	27.620	43.832
	0.6	14.019	22.846	27.665	44.027
	0.8	14.130	23.451	27.704	44.216
	1	14.250	24.166	27.738	44.406
5	0	13.777	21.783	27.554	43.566
	0.2	13.819	21.950	27.575	43.649
	0.4	13.905	22.309	27.616	43.816
	0.6	14.000	22.766	27.656	43.991
	0.8	14.099	23.314	27.690	44.158
	1	14.206	23.960	27.720	44.326
10	0	13.777	21.783	27.554	43.566
	0.2	13.817	21.944	27.574	43.646
	0.4	13.897	22.278	27.612	43.800
	0.6	13.983	22.694	27.648	43.958
	0.8	14.071	23.192	27.678	44.107
	1	14.167	23.779	27.704	44.255

plane mode for square FG micro/nano plates versus the length scale parameter is depicted in Fig. 1. The curves are plotted for the gradient indexes $\bar{\phi} = 1, 5$ and 10, and length-to-thickness ratios of 5 and 10. Similar curves are depicted in Fig. 2 for the in-plane mode. From Figs. 1 and 2, it is concluded that the non-dimensional frequencies increase by increasing the length scale parameter and/or by decreasing the gradient index. It is evident that the rate of increasing effect of length scale parameter is dropped rapidly when the length scale parameter takes very smaller values. Also, it is obvious that the effect of gradient index on the frequency of the out-of-plane mode decreases by increasing the length scale parameter. This trend is completely different for the frequency of the in-plane mode. In other words, the decreasing effect of gradient index on the frequency of the in-plane mode increases when the length scale parameter increases. It can be seen from Fig. 2 that for the small values of length scale parameter, the change of first frequency for the in-plane mode with the gradient index is negligible. In other words, the effect of gradient index on the shear stiffness is negligible when the length scale parameter is small.

Fig. 3(a) and (b) highlight the effect of thickness-to-length ratio on the first frequency of the out-of-plane mode for square FG micro/nano plates when the length scale parameter is set to 0 and 0.5, respectively. The curves are plotted for the gradient indexes $\bar{\phi} = 1, 5$ and 10. It can be seen that as the thickness-to-length ratio increases, the frequency decreases. The rate of decrease is very small for very thin plates. It is observed from Fig. 3b that for the nonzero value of length scale parameter, $\bar{l} = 0.5$, the decreasing effect of gradient index on the first frequency reduces when the thickness-to-length ratio increases, and is negligible for very thick plate $h/a \geqslant 0.4$. But, as Fig. 3(a) indicates, the decreasing effect of gradient index on the first frequency for $\bar{l} = 0$ is approximately constant for different thickness-to-length ratios of FG plate.

Variation of first non-dimensional frequency of the in-plane mode for square FG plates versus the thickness-to-length ratio is depicted in Fig. 4 for three different cases as homogeneous plate with the length scale parameter $\bar{l} = 0.5$, and FG plates with the gradient index $\bar{\phi} = 10$ and length scale parameters $\bar{l} = 0$ and 0.5. It can be observed that for these cases, frequency of the in-plane mode increases with a decrease in the thickness-to-length ratio. The rate of the increase rises sharply when the thickness-to-length ratio decreases. In other words, the first frequency of the in-plane mode is very high when the plate is very thin. This is due to the increase of the shear rigidity of plate.

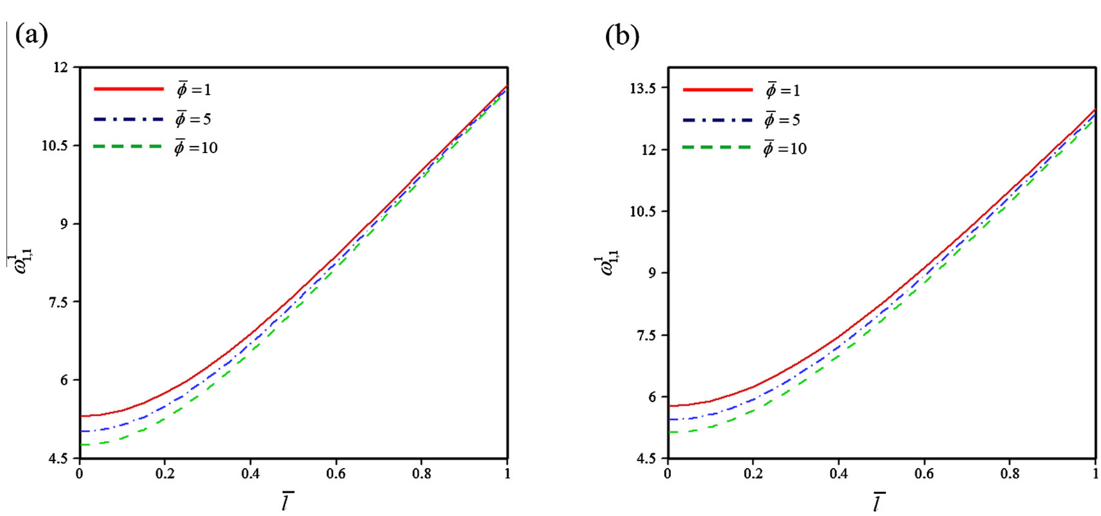

Fig. 1. Variation of first non-dimensional frequency for the out-of-plane mode with length scale parameter: (a) length-to-thickness of 5 and (b) length-to-thickness of 10.

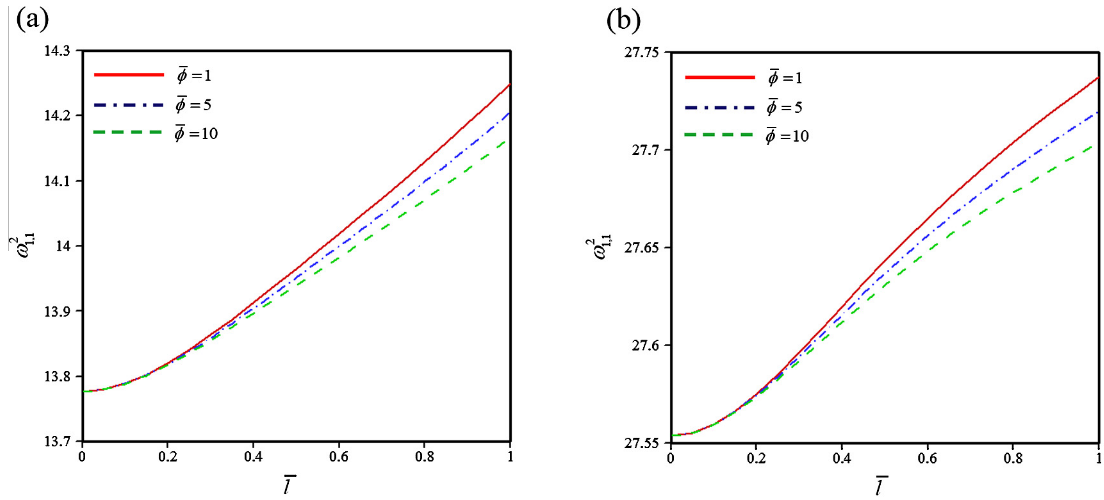

Fig. 2. Variation of first non-dimensional frequency for the in-plane mode with length scale parameter: (a) length-to-thickness of 5 and (b) length-to-thickness of 10.

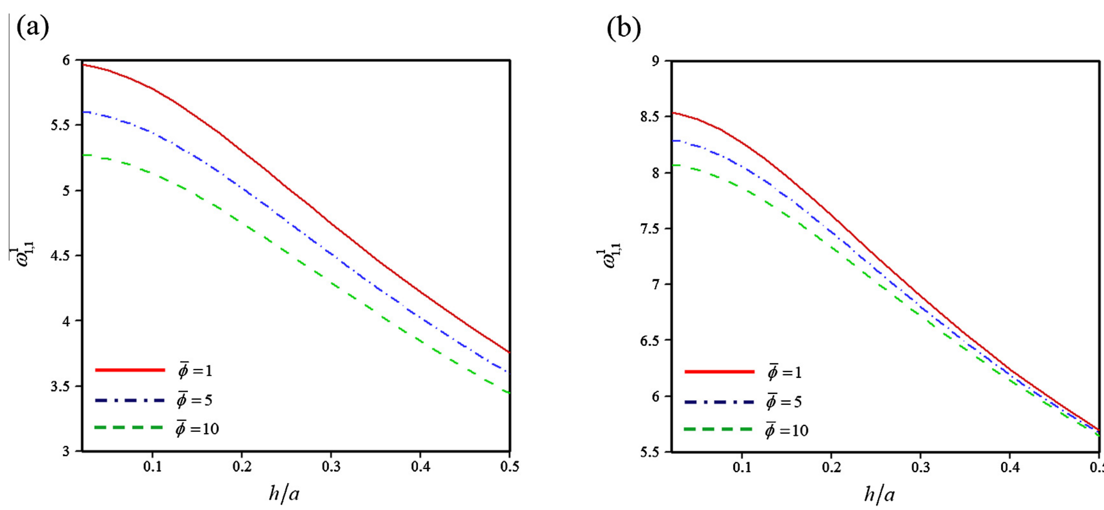

Fig. 3. Variation of first non-dimensional frequency for the out-of-plane mode versus the thickness-to-length ratio: (a) $\bar{l}=0$ and (b) $\bar{l}=0.5$.

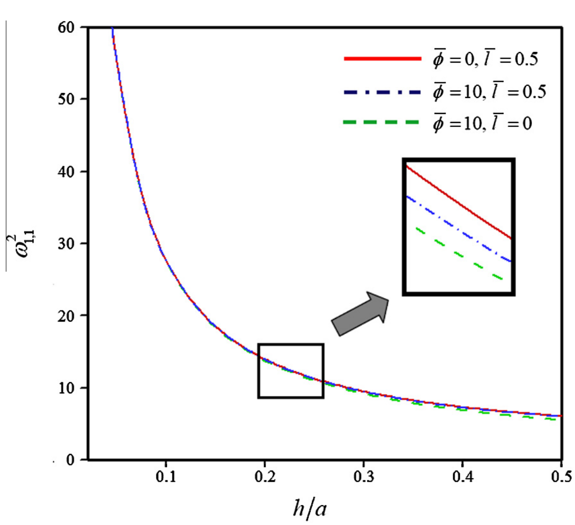

Fig. 4. Variation of first non-dimensional frequency for the in-plane mode versus the thickness-to-length ratio.

4. Conclusion

Based on the modified couple stress and three-dimensional elasticity theories, a new model is presented for bending and free vibration of FG micro/nano plates. Hamilton's principle is used to derive the equations of motion and associated boundary conditions. The developed model contains only one material length scale parameter to account micro/nano scale effect. Analytical solutions is presented for both in-plane and out-of-plane free vibration of FG micro/nano plates when the boundary conditions are simply supported. To solve the governing equations, elasticity modulus and mass density are assumed to change through the plate thickness based on the exponential law. The numerical examples are presented to investigate the influence of length scale parameter, material gradient index and thickness-to-length ratio on the frequencies of FG micro/nano plates. From the results, it is concluded that the inclusion of length scale parameter leads to an increase in the rigidity of the plate and consequently increasing the natural frequencies. This effect is very small for the frequencies of the in-plane modes when compared to the frequencies of the out-of-plane modes. Also, increasing the gradient index enhances the effect of length scale parameter on the frequencies of the out-of-plane modes, while it reduces the effect of length scale parameter on the frequencies of the in-plane modes.

References

[1] Toupin RA. Elastic materials with couple stresses. Arch Ration Mech Anal 1962;11:385–414.
[2] Mindlin RD, Tiersten HF. Effects of couple-stresses in linear elasticity. Arch Ration Mech Anal 1962;11:415–48.
[3] Mindlin RD. Influence of couple-stresses on stress concentrations. Exp Mech 1963;3:1–7.
[4] Koiter WT. Couple-stresses in the theory of elasticity: I and II. Proc K Ned Akad Wet. (B) 1964;67:17–44.
[5] Aifantis EC. Strain gradient interpretation of size effects. Int J Fractures 1999;95:1–4.
[6] Eringen AC. Nonlocal polar elastic continua. Int J Eng Sci 1972;10:1–16.
[7] Gurtin ME, Weissmuller J, Larche F. The general theory of curved deformable interfaces in solids at equilibrium. Philos Mag A 1998:1093–109.
[8] Yang F, Chong ACM, Lam DCC, Tong P. Couple stress based strain gradient theory for elasticity. Int J Solids Struct 2002;39:2731–43.
[9] Park SK, Gao XL. Bernoulli–Euler beam model based on a modified couple stress theory. J Micromech Microeng 2006;16:2355.
[10] Kong S, Zhou S, Nie Z, Wang K. The size-dependent natural frequency of Bernoulli–Euler microbeams. Int J Eng Sci 2008;46(5):427–37.
[11] Kahrobaiyan MH, Asghari M, Rahaeifard M, Ahmadian MT. Investigation of the size-dependent dynamic characteristics of atomic force microscope microcantilevers based on the modified couple stress theory. Int J Eng Sci 2010;48(12):1985–94.
[12] Ma HM, Gao XL, Reddy JN. A microstructure-dependent Timoshenko beam model based on a modified couple stress theory. J Mech Phys Solids 2008;56(12):3379–91.
[13] Fu Y, Zhang J. Modeling and analysis of microtubules based on a modified couple stress theory. Phys E: Low-Dimension Syst Nanostruct 2010;42(5):1741–5.
[14] Ke LL, Wang YS. Flow-induced vibration and instability of embedded double walled carbon nanotubes based on a modified couple stress theory. Phys E: Low-Dimension Syst Nanostruct 2011;43(5):1031–9.
[15] Ke LL, Wang YS, Wang ZD. Thermal effect on free vibration and buckling of size-dependent microbeams. Phys E: Low-Dimension Syst Nanostruct 2011;43(7):1387–93.
[16] Tsiatas GC. A new Kirchhoff plate model based on a modified couple stress theory. Int J Solids Struct 2009;46(13):2757–64.
[17] Yin L, Qian Q, Wang L, Xia W. Vibration analysis of microscale plates based on modified couple stress theory. Acta Mech Solida Sin 2010;23(5):386–93.
[18] Jomehzadeh E, Noori HR, Saidi AR. The size-dependent vibration analysis of micro plates based on a modified couple stress theory. Phys E: Low-Dimension Syst Nanostruct 2011;43(4):877–83.
[19] Akgoz B, Civalek O. Free vibration analysis for single-layered graphene sheets in an elastic matrix via modified couple stress theory. Mater Des 2012;42:164–71.
[20] Ma HM, Gao XL, Reddy JN. A non-classical Mindlin plate model based on a modified couple stress theory. Acta Mech 2011;220(1–4):217–35.
[21] Ke L-L, Wang Y-S, Yang J, Kitipornchai S. Free vibration of size-dependent Mindlin microplates based on the modified couple stress theory. J Sound Vib 2012;331(1):94–106.
[22] Witvrouw A, Mehta A. The use of functionally graded poly-SiGe layers for MEMS applications. Mater Sci Forum 2005;492–493:255–60.
[23] Lee Z, Ophus C, Fischer LM, Nelson-Fitzpatrick N, Westra KL, Evoy S, et al. Metallic NEMS components fabricated from nanocomposite Al–Mo films. Nanotechnol 2006;17:3063–70.
[24] Fu Y, Du H, Zhang S. Functionally graded TiN/TiNi shape memory alloy films. Mater Lett 2003;57:2995–9.
[25] Rahaeifard M, Kahrobaiyan MH, Ahmadian MT. Sensitivity analysis of atomic force microscope cantilever made of functionally graded materials. In: 3rd international conference on micro- and nanosystems. DETC2009-86254; 2009. p. 539–44.
[26] Asghari M, Ahmadian MT, Kahrobaiyan MH, Rahaeifard M. On the size dependent behavior of functionally graded micro-beams. Mater Des 2010;31(5):2324–9.
[27] Asghari M, Kahrobaiyan MH, Rahaeifard M, Ahmadian MT. The modified couple stress functionally graded Timoshenko beam formulation. Mater Des 2011;32(3):1435–46.
[28] Ke LL, Wang YS. Size effect on dynamic stability of functionally graded microbeams based on a modified couple stress theory. Compos Struct 2011;93(2):342–50.
[29] Ke LL, Wang YS, Yang J, Kitipornchai S. Nonlinear free vibration of size dependent functionally graded microbeams. Int J Eng Sci 2012;50(1):256–67.
[30] Reddy JN, Berry Jessica. Nonlinear theories of axisymmetric bending of functionally graded circular plates with modified couple stress. Compos Struct 2012;94(12):3664–8.
[31] Reddy JN, Kim J. A nonlinear modified couple stress-based third-order theory of functionally graded plates. Compos Struct 2012;94:1128–43.
[32] Kim J, Reddy JN. Analytical solutions for bending, vibration, and buckling of FGM plates using a couple stress-based third-order theory. Compos Struct 2013;103:86–98.
[33] Ke LL, Yang J, Kitipornchai S, Bradford MA. Bending, buckling and vibration of size-dependent functionally graded annular microplates. Compos Struct 2012;94:3250–7.
[34] Thai H-T, Choi D-H. Size-dependent functionally graded Kirchhoff and Mindlin plate models based on a modified couple stress theory. Compos Struct 2013;95:142–53.
[35] Thai H-T, Kim S-E. A size-dependent functionally graded Reddy plate model based on a modified couple stress theory. Compos Part B 2013;50:1636–45.
[36] Thai H-T, Vo TP. A size-dependent functionally graded sinusoidal plate model based on a modified couple stress theory. Compos Struct 2013;96:376–83.
[37] Simsek M, Reddy JN. Bending and vibration of functionally graded microbeams using a new higher order beam theory and the modified couple stress theory. Int J Eng Sci 2013;64:37–53.
[38] Jung WY, Han SCH, Park WT. A modified couple stress theory for buckling analysis of S-FGM nanoplates embedded in Pasternak elastic medium. Compos: Part B 2014;60:746–56.
[39] Jung WY, Park WT, Han SCH. Bending and vibration analysis of S-FGM microplates embedded in Pasternak elastic medium using the modified couple stress theory. Int J Mech Sci 2014;87:150–62.
[40] Ansari R, Faghih Shojaei M, Mohammadi V, Gholami R, Darabi MA. Nonlinear vibrations of functionally graded Mindlin microplates based on the modified couple stress theory. Compos Struct 2014;114:124–34.